Journal of the Optical Society of Korea, Vol 5, No. 3, September 2001, pp. 93-98

Performance of the Two-Stage Iterative Fourier Transform Algorithm for Designing Phase-Only Diffractive Pattern Elements

Phil Ho Jung and Doo Jin Cho*

Department of Physics, Ajou University, Suwon 442-749, KOREA

(Received May 25, 2001)

In order to verify the performance of the two-stage iterative Fourier transform algorithm[Hankook Kwanghak Hoeji **11**, 47 (2000)], a number of phase-only diffractive pattern elements which produce simple 16×16-pixel intensity patterns useful in the field of optical information processing have been designed and their performance has been compared with that from the nonlinear least-squares algorithm[Appl. Opt. **36**, 7297 (1997)] which is computationally intensive. For all intensity patterns, elements designed by the former algorithm show better overall signal-to-noise ratio and uniformity, although they show essentially the same diffraction efficiency. In the case of continuous phase elements, they show far superior uniformity. Computationally, the former algorithm is far more efficient than the latter.

OCIS codes : 050.1970, 090.1760, 090.1970, 140.3300, 200.4650.

I. INTRODUCTION

Diffractive optical elements(DOE's) which produce given intensity patterns via Fraunhofer diffraction are called diffractive pattern elements(DPE's), kinoforms and computer-generated Fourier holograms, and play an important role in optical signal processing, optical interconnects and laser material processing, etc. [1,2] Although numerous methods have been proposed for designing these kinds of DOE's, the iterative Fourier transform algorithm(IFTA) and its variants are most popular. Originally the IFTA proposed by Gerchberg and Saxton [3] was successfully applied to phase retrieval. Since the IFTA relies on the fast Fourier transform(FFT), it is computationally effective. However it has a well-known stagnation problem of falling into a local minimum, and various modified algorithms have been proposed to alleviate it. The hybrid input-output algorithms(HIOA's) proposed by Fienup [4] alleviate the stagnation problem with improved convergence.

Lin and Sawchuk [5] proposed the new Pnoise algorithm(NPA) which is an improved form of the two-stage algorithm with a dummy area [1,6]. The algorithm with a dummy area yields good results by loosening constraints, but has the disadvantage of low diffraction efficiency and an increased space-bandwidth product. In the NPA, the constraints on the noise diffraction orders are loosened instead of introducing a dummy area, i.e., the intensity of the noise orders are restricted by a threshold. Updating the threshold adaptively according to the signal-to-noise ratio(SNR), the SNR and the diffraction efficiency are optimized. Chen and Sawchuk [7] developed a nonlinear least-squares algorithm(NLSA) which used a phase-shifting quantization procedure. Although it is computationally intensive due to the cost of numerical generation of the Jacobian matrix, the NLSA produces uniform, power-efficient DOE's that have a very good SNR, superior in most criteria to those designed by the two-stage iterative Fourier transform algorithm of Wyrowski [1].

We proposed a two-stage algorithm [8] designated as the NPA-HIOA which is based both on the NPA and the HIOA. It has been found that the NPA-HIOA yields DPE designs with improved convergence which show good SNR, uniformity and diffraction efficiency even for complicated grayscale intensity patterns. In this work, the performance of the NPA-HIOA is compared with that of the NLSA for a number of phase-only DPE's which produce three 16×16-pixel intensity patterns useful in the field of optical information processing. In Section 2, diffraction theory of diffractive pattern elements is presented briefly, and several performance criteria for design algorithms are defined. In Section 3, the NPA-HIOA is explained briefly. In Section 4, numerical results of the NPA-HIOA are compared with those of the NLSA.

II. DIFFRACTION THEORY OF DIFFRACTIVE PATTERN ELEMENTS

In the scalar diffraction regime, the complex amplitude transmittance function of a diffractive phase element of P periods is given by

$$g(x) = \sum_{p=0}^{P-1} \sum_{q=0}^{Q-1} g(q\Delta x) rect(\frac{x - q\Delta x - pQ\Delta x}{\Delta x}), \quad (1)$$

where $g(q\Delta x) = \exp[i\phi(q\Delta x)]$, $rect(x)$ is a rectangle function, Δx is the pixel size, and Q is the number of pixels within a period. Note that one-dimensional version of the complex amplitudes are presented in order to simplify the notation.

The normalized complex amplitude in the diffraction plane is given by the Fourier transform of $g(x)$

$$G(K) = \frac{1}{PQ} \text{sinc}\left(\frac{K}{Q}\right) \frac{\sin(\pi PK)}{\sin(\pi K)} \times \sum_{q=0}^{Q-1} g(q\Delta x) \exp\left(-i2\pi \frac{q}{Q} K\right), \quad (2)$$

where $K = Qf\Delta x$ (f is the spatial frequency) and sinc(x)= $\sin(\pi x)/(\pi x)$. The normalized intensity is given by $|G|^2$. The summation portion of Eq. (2) is the discrete Fourier transform(DFT) of g, and is denoted by $\bar{G}$

$$\bar{G}(m) = DFT(g(q\Delta x)), \quad (3)$$

where the diffraction order m denotes the integer value of K.

The above equations can be readily generalized to two-dimensional ones. For each diffraction order (m, n) it is desired that the normalized intensity $\eta_{mn} = |G(m,n)|^2$ is as close to the given intensity pattern denoted by $I(m, n) = I_{mn}$ as possible. We designate the signal region(the given intensity is not zero) as S_s, and the noise region(the given intensity is zero) S_n. As performance criteria of algorithms, we employ the minimum SNR $SNRmin$, the Uniformity U, diffraction efficiency η, diffraction efficiency with respect to the signal area η_w, and root-mean-squared error $RMSE$ defined as follows:

$$SNRmin = 10log_{10} \frac{\eta_{smin}}{\eta_{nmax}} \quad (4)$$

$$U = \frac{\eta_{smax} - \eta_{smin}}{\eta_{smax} + \eta_{smin}} \quad (5)$$

$$\eta = \sum_{(m,n)\in S_s} \eta_{mn} \quad (6)$$

$$\eta_w = \frac{\sum_{(m,n)\in S_s} \eta_{mn}}{\sum_{(m,n)\in S_s} \eta_{mn} + \sum_{(m,n)\in S_n} \eta_{mn}} \quad (7)$$

$$RMSE = \sqrt{\sum_{m,n} (I(m,n) - \eta_{mn})^2}, \quad (8)$$

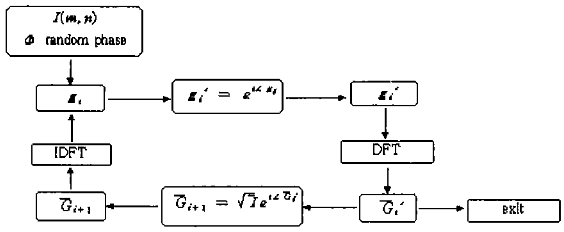

FIG. 1. Schematics of the iterative Fourier transform algorithm.

where η_{smax} and η_{smin} are the maximum and the minimum of η_{mn} in S_s normalized by I_{mn}, respectively and η_{nmax} is the maximum of η_{mn} in S_n.

III. TWO-STAGE ITERATIVE FOURIER TRANSFORM ALGORITHM

The basic IFTA is schematically shown in Fig. 1. The initial value g_0 of the iterative loop is obtained from the inverse DFT of the initial complex amplitude $\bar{G}_0$ which is given by $\bar{G}_0 = \sqrt{\bar{I}} \exp(i\Phi)$, where $\bar{I}$ denotes the given intensity pattern divided by sinc^2 functions(See Eq. (2)) and Φ the random phase. In the iterative loop, the object-domain constraint requires that the magnitude of g_i' be uniform, i.e., g_i' be the phasor of g_i. Fourier-domain constraints are fulfilled by setting the magnitude of $\bar{G}_{i+1}$ to be $\sqrt{\bar{I}}$.

In the HIOA the input $\bar{G}_{i+1}$ to the iterative loop does not have to satisfy Fourier-domain constraints as in the IFTA. It is modified so that the output $\bar{G}_i'$ quickly converges to what is desired. In other words $\bar{G}_{i+1}$ is modified so that the deviation of the output $\bar{G}_i'$ from Fourier-domain constraints is reflected in the input. In this work, the procedure shown in Fig. 1 is followed with the change in Fourier-domain constraints:

$$\bar{G}_{i+1} = [|\bar{G}_i| + \beta(\sqrt{\bar{I}} - |\bar{G}_i'|)] \exp(i\angle\bar{G}_i'), \quad (9)$$

where β is a constant that reflects the deviation of $|\bar{G}_i'|$ from $\sqrt{\bar{I}}$ in the input. According to our experience, $\beta = 0.05$ yields better results than the IFTA in most cases. Note that there are other choices than Eq. (9) which yield satisfactory results.

In the NPA, the constraints on the noise diffraction orders are loosened, i.e., the intensity of the noise orders are restricted by a threshold which is adaptively updated according to the SNR. In the first stage, the IFTA is used to determine a continuous phase distribution. At the second stage, it introduces thresholding to the noise region S_n and employs the stepwise phase quantization in the iterative loop. For the signal region S_s Fourier-domain constraints are the same as in the IFTA. In the noise region, $\bar{\eta}_{mn} = |\bar{G}(m,n)|^2$ is thresholded by α defined below:

$$S_s \;:\; \bar{G}_{i+1} = \sqrt{\bar{I}}\exp(i\angle\bar{G}'_i) \tag{10}$$

$$S_n \;:\; \bar{G}_{i+1} = \begin{cases} \sqrt{\alpha}\exp(i\angle\bar{G}'_i) & ,\ \bar{\eta}_{mn} \geq \alpha \\ \bar{G}'_i & ,\ \bar{\eta}_{mn} < \alpha \end{cases} \tag{11}$$

$$\alpha = \frac{\bar{\eta}_{smin}}{10^{limit}/10} \tag{12}$$

$$limit = \min(\max SNRmin, \overline{SNRmin} + 4), \tag{13}$$

where $\max SNRmin$ is a target parameter introduced to optimize $SNRmin$, $\bar{\eta}_{smin}$ is the minimum of $\bar{\eta}_{mn}$ in S_s normalized by $\bar{I}_{mn}$, and $\overline{SNRmin}$ is defined by Eq. (4) with η_{smin} replaced by $\bar{\eta}_{smin}$ and η_{nmax} by $\bar{\eta}_{nmax}$ which is the maximum of $\bar{\eta}_{mn}$ in S_n.

The two-stage algorithm designated as the NPA-HIOA which is based both on the NPA and the HIOA uses the HIOA of Eq. (9) in the first stage, in order to determine a continuous phase distribution with improved convergence. At the second stage, it combines the NPA with the HIOA and introduces the stepwise phase quantization. [1] For the signal region S_s, we employ Eq. (9) of the HIOA hoping that the advantage of fast convergence remains. However, for the noise region S_n, we follow the NPA, i.e., Eqs. (11), (12) and (13) are used. It is desired that the advantages of the NPA, such as high SNR, good uniformity and high diffraction efficiency remain the same by loosening Fourier-domain constraints on the noise region.

In the second stage we introduce the stepwise phase quantization in the iterative loop in order to obtain an optimal quantized phase distribution. It is found that we can not avoid premature stagnation if plain quantization is employed in the iterative loop. In the stepwise phase quantization the range of quantization is extended stepwise. When the phase $\angle g_i$ is within the range, it is quantized according to object-domain constraints. Otherwise we keep the phase value. In this work the second stage is divided into ten steps of quantization. We keep the iteration number for each step the same except for the final step. It is found that, in most cases, it is not worthwhile to iterate with the full range of quantization. In other words no improvement is obtained in the final step of quantization.

IV. PERFORMANCE OF DPE DESIGNS

The NPA-HIOA is used to design a number of DPE's which have both continuous and quantized phase and produce 16×16-pixel intensity patterns via Fraunhofer diffraction. Three intensity patterns shown in Fig. 2, i.e., (a) [1, 2, 4] cellular hypercube interconnection pattern, (b) 3×3 uniform spot array, and (c) 4:2:1 weighted-analog interconnection pattern with nine fan-outs, which are important in the field of optical information processing have been considered. The cellular hypercube interconnection pattern is useful for parallel optical cellular-logic processing, uniform spot array for illuminating an array of optical modulators, and the 4:2:1 weighted-analog interconnection pattern is used in a three-layer optical neural-network system.

The performance of these DPE's are compared to those designed by the NLSA. Simulation results for the NLSA are taken from ref. [7]. Note that, in ref. [7], definitions of the SNRmin and the Uniformity are slightly different from Eqs.(4) and (5), respectively due to the difference in definitions of η_{smax} and η_{smin}. In the present work these differences only matter in non-uniform intensity patterns, i.e., the 4:2:1 weighted-analog interconnection pattern. Since, according to definitions in ref. [7], η_{smax} and η_{smin} tend to be located near the maximum and the minimum of I_{mn}, respectively, it is clear that definitions in the present work are more appropriate.

In the first stage of the NPA-HIOA, the iteration number is 40. The second stage involves 10 steps of stepwise phase quantization, as noted above. Each step except for the last consists of 15 iterations, and the last step just a single loop. Thus the iteration number of the second stage is 136. In this work the total number of initial guesses for NPA-HIOA is 40: two values of β(0.1,0.05), five values of $\max SNRmin$(12, 14, 16, 18, 20) and four of initial random phase. Note that these values of β and $\max SNRmin$ have produced excellent designs in many different intensity patterns. We have also referred to the $SNRmin$ values obtained from the NLSA. In evaluating the performance of designs, the uniformity has been the major criterion. Quantized DPE's of 4, 8, 16, 32, and 64 phase levels as well as DPE's with continuous phase have been designed. Note that we use a high-level language, Scilab [9] in programming the NPA-HIOA.

1. [1, 2, 4] cellular hypercube interconnection pattern

In Table 1, performance criteria for the NPA-HIOA and NLSA are summarized for the case of [1, 2, 4] cellular hypercube interconnection pattern shown in

$$I = \left|\begin{array}{cccccccccccccccc}
0 & 0 & 0 & 0 & 0 & 0 & 0 & 0 & 0 & 0 & 0 & 0 & 0 & 0 & 0 & 0 \\
0 & 0 & 0 & 0 & 0 & 0 & 0 & 0 & 0 & 0 & 0 & 0 & 0 & 0 & 0 & 0 \\
0 & 0 & 0 & 0 & 0 & 0 & 0 & 0 & 0 & 0 & 0 & 0 & 0 & 0 & 0 & 0 \\
0 & 0 & 0 & 0 & 0 & 0 & 0 & 0 & 0 & 0 & 0 & 0 & 0 & 0 & 0 & 0 \\
0 & 0 & 0 & 0 & 0 & 0 & 0 & 0 & 1 & 0 & 0 & 0 & 0 & 0 & 0 & 0 \\
0 & 0 & 0 & 0 & 0 & 0 & 0 & 0 & 0 & 0 & 0 & 0 & 0 & 0 & 0 & 0 \\
0 & 0 & 0 & 0 & 0 & 0 & 0 & 0 & 1 & 0 & 0 & 0 & 0 & 0 & 0 & 0 \\
0 & 0 & 0 & 0 & 0 & 0 & 0 & 0 & 1 & 0 & 0 & 0 & 0 & 0 & 0 & 0 \\
0 & 0 & 0 & 0 & 1 & 0 & 1 & 1 & 0 & 1 & 1 & 0 & 1 & 0 & 0 & 0 \\
0 & 0 & 0 & 0 & 0 & 0 & 0 & 0 & 1 & 0 & 0 & 0 & 0 & 0 & 0 & 0 \\
0 & 0 & 0 & 0 & 0 & 0 & 0 & 0 & 1 & 0 & 0 & 0 & 0 & 0 & 0 & 0 \\
0 & 0 & 0 & 0 & 0 & 0 & 0 & 0 & 0 & 0 & 0 & 0 & 0 & 0 & 0 & 0 \\
0 & 0 & 0 & 0 & 0 & 0 & 0 & 0 & 1 & 0 & 0 & 0 & 0 & 0 & 0 & 0 \\
0 & 0 & 0 & 0 & 0 & 0 & 0 & 0 & 0 & 0 & 0 & 0 & 0 & 0 & 0 & 0 \\
0 & 0 & 0 & 0 & 0 & 0 & 0 & 0 & 0 & 0 & 0 & 0 & 0 & 0 & 0 & 0 \\
0 & 0 & 0 & 0 & 0 & 0 & 0 & 0 & 0 & 0 & 0 & 0 & 0 & 0 & 0 & 0
\end{array}\right| \times 1/12$$

(a)

$$I = \left|\begin{array}{cccccccccccccccc}
0 & 0 & 0 & 0 & 0 & 0 & 0 & 0 & 0 & 0 & 0 & 0 & 0 & 0 & 0 & 0 \\
0 & 0 & 0 & 0 & 0 & 0 & 0 & 0 & 0 & 0 & 0 & 0 & 0 & 0 & 0 & 0 \\
0 & 0 & 0 & 0 & 0 & 0 & 0 & 0 & 0 & 0 & 0 & 0 & 0 & 0 & 0 & 0 \\
0 & 0 & 0 & 0 & 0 & 0 & 0 & 0 & 0 & 0 & 0 & 0 & 0 & 0 & 0 & 0 \\
0 & 0 & 0 & 0 & 0 & 0 & 0 & 0 & 0 & 0 & 0 & 0 & 0 & 0 & 0 & 0 \\
0 & 0 & 0 & 0 & 0 & 0 & 0 & 0 & 0 & 0 & 0 & 0 & 0 & 0 & 0 & 0 \\
0 & 0 & 0 & 0 & 0 & 0 & 0 & 0 & 0 & 0 & 0 & 0 & 0 & 0 & 0 & 0 \\
0 & 0 & 0 & 0 & 0 & 0 & 0 & 1 & 1 & 1 & 0 & 0 & 0 & 0 & 0 & 0 \\
0 & 0 & 0 & 0 & 0 & 0 & 0 & 1 & 1 & 1 & 0 & 0 & 0 & 0 & 0 & 0 \\
0 & 0 & 0 & 0 & 0 & 0 & 0 & 1 & 1 & 1 & 0 & 0 & 0 & 0 & 0 & 0 \\
0 & 0 & 0 & 0 & 0 & 0 & 0 & 0 & 0 & 0 & 0 & 0 & 0 & 0 & 0 & 0 \\
0 & 0 & 0 & 0 & 0 & 0 & 0 & 0 & 0 & 0 & 0 & 0 & 0 & 0 & 0 & 0 \\
0 & 0 & 0 & 0 & 0 & 0 & 0 & 0 & 0 & 0 & 0 & 0 & 0 & 0 & 0 & 0 \\
0 & 0 & 0 & 0 & 0 & 0 & 0 & 0 & 0 & 0 & 0 & 0 & 0 & 0 & 0 & 0 \\
0 & 0 & 0 & 0 & 0 & 0 & 0 & 0 & 0 & 0 & 0 & 0 & 0 & 0 & 0 & 0 \\
0 & 0 & 0 & 0 & 0 & 0 & 0 & 0 & 0 & 0 & 0 & 0 & 0 & 0 & 0 & 0
\end{array}\right| \times 1/9$$

(b)

$$I = \left|\begin{array}{cccccccccccccccc}
0 & 0 & 0 & 0 & 0 & 0 & 0 & 0 & 0 & 0 & 0 & 0 & 0 & 0 & 0 & 0 \\
0 & 0 & 0 & 0 & 0 & 0 & 0 & 0 & 0 & 0 & 0 & 0 & 0 & 0 & 0 & 0 \\
0 & 0 & 0 & 0 & 0 & 0 & 0 & 0 & 0 & 0 & 0 & 0 & 0 & 0 & 0 & 0 \\
0 & 0 & 0 & 0 & 0 & 0 & 0 & 0 & 0 & 0 & 0 & 0 & 0 & 0 & 0 & 0 \\
0 & 0 & 0 & 0 & 0 & 0 & 0 & 0 & 0 & 0 & 0 & 0 & 0 & 0 & 0 & 0 \\
0 & 0 & 0 & 0 & 0 & 0 & 0 & 0 & 0 & 0 & 0 & 0 & 0 & 0 & 0 & 0 \\
0 & 0 & 0 & 0 & 0 & 0 & 0 & 0 & 0 & 0 & 0 & 0 & 0 & 0 & 0 & 0 \\
0 & 0 & 0 & 0 & 0 & 0 & 0 & 1 & 2 & 1 & 0 & 0 & 0 & 0 & 0 & 0 \\
0 & 0 & 0 & 0 & 0 & 0 & 0 & 2 & 4 & 2 & 0 & 0 & 0 & 0 & 0 & 0 \\
0 & 0 & 0 & 0 & 0 & 0 & 0 & 1 & 2 & 1 & 0 & 0 & 0 & 0 & 0 & 0 \\
0 & 0 & 0 & 0 & 0 & 0 & 0 & 0 & 0 & 0 & 0 & 0 & 0 & 0 & 0 & 0 \\
0 & 0 & 0 & 0 & 0 & 0 & 0 & 0 & 0 & 0 & 0 & 0 & 0 & 0 & 0 & 0 \\
0 & 0 & 0 & 0 & 0 & 0 & 0 & 0 & 0 & 0 & 0 & 0 & 0 & 0 & 0 & 0 \\
0 & 0 & 0 & 0 & 0 & 0 & 0 & 0 & 0 & 0 & 0 & 0 & 0 & 0 & 0 & 0 \\
0 & 0 & 0 & 0 & 0 & 0 & 0 & 0 & 0 & 0 & 0 & 0 & 0 & 0 & 0 & 0 \\
0 & 0 & 0 & 0 & 0 & 0 & 0 & 0 & 0 & 0 & 0 & 0 & 0 & 0 & 0 & 0
\end{array}\right| \times 1/16$$

(c)

FIG. 2. (a) [1, 2, 4] cellular hypercube interconnection pattern (b) 3×3 uniform spot array (c) 4:2:1 weighted-analog interconnection pattern.

Fig. 2(a). DPE's designed by NPA-HIOA show better overall performance, especially in $SNRmin$ and uniformity, although they yield essentially the same diffraction efficiency. Especially the uniformity for the case of the continuous phase(CP) is extremely good. Values of β and max$SNRmin$ which yield the best uniformity in each Z(number of phase levels) are as follows: for Z=4, β=0.1, max$SNRmin$=14; for Z=8, β=0.05, max$SNRmin$=16; for Z=16, β=0.05, max$SNRmin$=14; for Z=32, β=0.1, max$SNRmin$=12; for Z=64, β=0.05, max $SNRmin$=16; for Z=CP, β=0.05, max$SNRmin$

TABLE 1. Performance of DPE designs which produce [1, 2, 4] cellular hypercube interconnection pattern.(CP denotes continuous phase.)

Method of DOE Design	Phase Levels Z	U(%)	η_w(%)	η(%)	$SNRmin$(dB)	Number of Initial Guesses
NPA-HIOA	4	1.53	80.08	66.19	11.05	40
	8	0.85	89.67	77.92	14.36	40
	16	0.10	91.15	80.82	15.15	40
	32	0.21	92.38	82.01	12.70	40
	64	0.20	91.46	81.02	15.71	40
	CP	0.0029	92.33	81.99	14.48	40
NLSA	4	2.92	81.84	67.69	9.66	100
	8	1.16	89.89	77.91	13.51	40
	16	0.25	91.91	81.05	13.81	20
	32	0.25	91.91	81.05	13.81	20
	64	0.25	91.91	81.05	13.81	20
	CP	0.25	91.91	81.05	13.81	20

TABLE 2. Performance of DPE designs which produce 3×3 uniform spot array.(CP denotes continuous phase.)

Method of DOE Design	Phase Levels Z	U(%)	η_w(%)	η(%)	$SNRmin$(dB)	Number of Initial Guesses
NPA-HIOA	4	2.81	81.08	74.87	11.73	40
	8	1.15	92.08	87.66	16.54	40
	16	0.56	93.72	90.54	18.01	40
	32	0.46	94.49	91.69	18.15	40
	64	0.20	94.63	91.98	18.12	40
	CP	0.0149	93.85	90.38	19.89	40
NLSA	4	1.59	81.56	75.61	10.12	40
	8	1.00	92.08	87.67	16.46	40
	16	0.99	94.17	91.10	16.31	40
	32	0.51	94.70	91.69	17.28	20
	64	0.34	94.79	91.78	18.04	20
	CP	0.19	94.85	91.74	18.33	20

=14. Although max$SNRmin$=12 gives the best uniformity of 0.0025% with $SNRmin$=12.50 in the case of Z=CP, we chose max$SNRmin$=14 because of a much higher $SNRmin$. Note that the reason why $SNRmin$ for Z=32 (NPA-HIOA) is lower is that max $SNRmin$=12 has been used in order to obtain the best uniformity.

2. 3×3 uniform spot array

In Table 2, performance criteria for the NPA-HIOA and NLSA are summarized for the case of 3×3 uniform spot array shown in Fig. 2(b). As the case of the cellular hypercube, DPE's designed by NPA-HIOA show better overall performance, especially in $SNRmin$ and uniformity, although they yield essentially the same diffraction efficiency. Uniformities for Z=4 and 8 are slightly worse. Values of β and max$SNRmin$ which yield the best uniformity and $SNRmin$ in each Z are as follows: for Z=4, β=0.05, max$SNRmin$=10; for Z=8, β=0.05, max$SNRmin$=16; for Z=16, β=0.05, max$SNRmin$=18; for Z=32, β=0.1, max$SNRmin$=18; for Z=64, β=0.1, max $SNRmin$=18; for Z=CP, β=0.1, max$SNRmin$=20.

In the cases of Z=32 and 64, max$SNRmin$=16 yields the best uniformity of 0.35% and 0.18% with lower $SNRmin$=16.75 and 16.73, respectively. For Z=CP, max$SNRmin$=14 yields the best uniformity of 0.0019% with significantly lower $SNRmin$=15.29. Note that values of max$SNRmin$ are greater than the case of the cellular hypercube, except for Z=4. Thus $SNRmin$'s are higher.

3. 4:2:1 weighted-analog interconnection pattern with nine fan-outs

In Table 3, performance criteria for the NPA-HIOA and NLSA are summarized for the case of the 4:2:1 weighted-analog interconnection pattern with nine fan-outs shown in Fig. 2(c). As the case of cellular hypercube and uniform spot array, DPE's designed by NPA-HIOA show better overall performance, especial-

TABLE 3. Performance of DPE designs which produce 4:2:1 weighted-analog interconnection pattern.(CP denotes continuous phase.)

Method of DOE Design	Phase Levels Z	U(%)	η_w(%)	η(%)	$SNRmin$(dB)	Number of Initial Guesses
NPA-HIOA	4	2.76	84.28	78.79	15.38	40
	8	1.39	89.55	85.92	14.23	40
	16	0.56	91.64	88.78	19.38	40
	32	0.27	92.27	89.66	19.37	40
	64	0.16	92.63	90.29	17.01	40
	CP	0.0014	93.27	91.40	18.53	40
NLSA	4	3.47	85.68	80.62	10.26	100
	8	1.58	90.16	86.71	11.39	40
	16	1.05	92.66	90.17	12.37	40
	32	0.55	93.27	90.88	13.88	20
	64	0.65	93.40	91.13	14.10	20
	CP	0.65	93.40	91.13	14.10	20

ly in $SNRmin$ and uniformity. The considerable improvement in $SNRmin$'s compared with other intensity patterns is partly due to the difference in the definition of η_{smin}. Note that diffraction efficiency is consistently slightly lower. Values of β and max$SNRmin$ which yield the best uniformity in each Z are as follows: for Z=4, β=0.1, max$SNRmin$=16; for Z=8, β=0.05, max$SNRmin$=14; for Z=16, β=0.05, max$SNRmin$=20; for Z=32, β=0.1, max$SNRmin$=20; for Z=64, β=0.05, max $SNRmin$=16; for Z=CP, β=0.05, max$SNRmin$=18. As the case of the uniform spot array, values of max$SNRmin$ are greater than the case of the cellular hypercube and thus $SNRmin$'s are higher.

In the case of the cellular hypercube which has a smaller noise region than other intensity patterns $SNRmin$'s are considerably lower overall, except for small Z's. The reason is that NPA-HIOA uses the noise region in loosening constraints in order to improve the performance, as noted in ref. [8].

It is interesting to compare DPE's designed by NPA-HIOA with those designed by the two-stage iterative Fourier transform algorithm of Wyrowski [7]. They are far superior in uniformity and $SNRmin$, but slightly inferior in diffraction efficiency. Note that the number of initial guesses in Wyrowski's algorithm was 500 which is more than twelve times that of NPA-HIOA.

As noted in the introduction, the NLSA is computationally intensive due to the cost of numerical generation of the Jacobian matrix. For the square array of dimension N, the cost in each iteration is of the order of $N^4 log_2 N^2$. Thus the NLSA is not useful for moderate N, such as 256 or 512 due to the enormous computational burden. Presumably this is the reason why only small intensity patterns have been designed using it. On the other hand, the numerical cost for the NPA-HIOA is mostly in the fast Fourier transform, which has the cost of the order of $N^2 log_2 N^2$. In the case of 16×16-pixel intensity pattens, the cost of NLSA is approximately 256 times that of NPA-HIOA for each iteration.

V. CONCLUSION

The two-stage iterative Fourier transform algorithm, NPA-HIOA that is based on both the HIOA and the NPA produces excellent designs for both continuous and quantized diffractive phase elements which yield given intensity patterns via Fraunhofer diffraction. It has the advantages of the NPA, such as high SNR, good uniformity and high diffraction efficiency, as well as good convergence which is the advantage of the HIOA.

In order to verify the performance of the NPA-HIOA, a number of phase-only DPE's which produce three simple 16×16-pixel intensity patterns useful in the field of optical information processing have been designed and their performance is compared with that from the nonlinear least-squares algorithm which uses a phase-shifting quantization procedure. The total number of initial guesses is 40 and the total iteration number is 176 with 10 steps of stepwise phase quantization in the second stage. For all intensity patterns, elements designed by the former algorithm show better signal-to-noise ratio and uniformity, although they show essentially the same diffraction efficiency. In the case of continuous phase elements, they show far superior uniformity. Computationally the former algorithm is far more efficient than the latter, especially for large arrays.

VI. ACKNOWLEDGMENTS

This work was supported by Korea Research Foundation Grant(KRF-99-015-DI0044).

*Corresponding author : djcho@ajou.ac.kr.

REFERENCES

[1] F. Wyrowski, J. Opt. Soc. Am. A **7**, 961 (1990).
[2] C. Haupt, M. Pahlke, R. Krupka, and H. J. Tiziani, Appl. Opt. **36**, 4411 (1997).
[3] R. W. Gerchberg and W. O. Saxton, Optik **35**, 237 (1972).
[4] J. R. Fienup, Opt. Eng. **19**, 297 (1980).
[5] J. Lin and A. A. Sawchuk, Appl. Opt. **36**, 3155 (1997).
[6] H. Akahori, Appl. Opt. **25**, 802 (1986).
[7] C. Chen and A. A. Sawchuk, Appl. Opt. **36**, 7297 (1997).
[8] Phil Ho Jung and Doo Jin Cho, Hankook Kwanghak Hoeji **11**, 47 (2000).
[9] http://www-rocq.inria.fr/scilab/